Joint interpretation of AER/FGF and ZPA/SHH over time and space underlies *hairy2* expression in the chick limb

Caroline J. Sheeba[1,2], Raquel P. Andrade[1,*] and Isabel Palmeirim[2,*,‡]

[1]Life and Health Sciences Research Institute (ICVS), School of Health Sciences, University of Minho, 4710-057 Braga, Portugal; ICVS/3B's - PT Government Associate Laboratory, Braga/Guimarães, Portugal
[2]Regenerative Medicine Program, Departamento de Ciências Biomédicas e Medicina, Universidade do Algarve, 8005-139 Faro, Portugal; IBB-Institute for Biotechnology and Bioengineering, Centro de Biomedicina Molecular e Estrutural, Universidade do Algarve, 8005-139 Faro, Portugal

*These authors contributed equally to this work
‡Author for correspondence (imesteves@ualg.pt; ipalmeirim@gmail.com)

Biology Open 1, 1102–1110
doi: 10.1242/bio.20122386
Received 26th June 2012
Accepted 11th July 2012

Summary

Embryo development requires precise orchestration of cell proliferation and differentiation in both time and space. A molecular clock operating through gene expression oscillations was first described in the presomitic mesoderm (PSM) underlying periodic somite formation. Cycles of *HES* gene expression have been further identified in other progenitor cells, including the chick distal limb mesenchyme, embryonic neural progenitors and both mesenchymal and embryonic stem cells. In the limb, *hairy2* is expressed in the distal mesenchyme, adjacent to the FGF source (AER) and along the ZPA-derived SHH gradient, the two major regulators of limb development. Here we report that *hairy2* expression depends on joint AER/FGF and ZPA/SHH signaling. FGF plays an instructive role on *hairy2*, mediated by Erk and Akt pathway activation, while SHH acts by creating a permissive state defined by Gli3-A/Gli3-R>1. Moreover, we show that AER/FGF and ZPA/SHH present distinct temporal and spatial signaling properties in the distal limb mesenchyme: SHH acts at a long-term, long-range on *hairy2*, while FGF has a short-term, short-range action. Our work establishes limb *hairy2* expression as an output of integrated FGF and SHH signaling in time and space, providing novel clues for understanding the regulatory mechanisms underlying *HES* oscillations in multiple systems, including embryonic stem cell pluripotency.

Key words: Fibroblast growth factor, HES expression, Limb development, Sonic hedgehog

Introduction

Periodic events underlie many aspects of our lives and some cell molecular oscillators have already been characterized and revealed to be crucial in insuring that the genetic/biochemical/morphological processes occur in their optimal temporal niche. One of such oscillators is the embryonic HES (Hairy/Enhancer of split)-based molecular clock (Pourquié, 2011) which was firstly identified by describing cyclic expression of avian *hairy1/2* genes during timely somite formation (Palmeirim et al., 1997; Jouve et al., 2000). Since then, this molecular oscillator has been described in multiple animal models (Andrade et al., 2007; Krol et al., 2011) and in a great variety of cells, including limb chondrogenic precursor cells (Pascoal et al., 2007; Aulehla and Pourquié, 2008), embryonic neural progenitors (Shimojo et al., 2008) and both mesenchymal (William et al., 2007) and embryonic stem cells (Kobayashi et al., 2009). Furthermore, major signaling pathways such as Notch, Wnt and FGF have been implicated in the molecular clock machinery (Dequéant et al., 2006; Krol et al., 2011; Pourquié, 2011). Mutations in genes associated with this oscillator underlie vertebral human malformations (Andrade et al., 2007; Pourquié, 2011; Sparrow et al., 2012), revealing that a tight regulation of HES biological activity is crucial for normal embryogenesis. Interestingly, many of these congenital anomalies also include limb defects (Andrade et al., 2007; Turnpenny et al., 2007; Sparrow et al., 2012).

The developing limb begins as a small bud of homogenous mesenchymal cells and gets sculptured into a 3D adult limb through coordinated growth and patterning. FGFs produced by the distal apical ectodermal ridge (AER) dictate proximal–distal (PD) outgrowth and maintain the distal limb mesenchyme cells in an undifferentiated, proliferative state, mediated by Erk/MAPK and Akt/PI3K pathways (Kawakami et al., 2003; Corson et al., 2003; Towers and Tickle, 2009). SHH produced by the zone of polarizing activity (ZPA) located at the posterior distal margin of the limb bud, governs anterior–posterior (AP) patterning (Riddle et al., 1993; Towers and Tickle, 2009). This is mediated through a SHH-dependent posterior-to-anterior gradient of Gli activator levels and an opposing Gli repressor gradient (Wang et al., 2000; Ahn and Joyner, 2004). In the chick distal-most limb mesenchyme, *hairy2* is cyclically expressed with a 6 hour periodicity (Pascoal et al., 2007; Aulehla and Pourquié, 2008), whereas it is permanently expressed in the posterior limb region

overlapping the ZPA and is absent from the anterior limb. The distal limb *hairy2*-expression domain is in close proximity with the FGF-producing AER and the ZPA/SHH source, the two primary signaling centers governing limb development. Importantly, during somitogenesis HES genes have been reported to be regulated in a Notch-independent manner by FGF (Niwa et al., 2007) and the time-period of their oscillations is influenced by SHH, most likely through modulation of Gli activity levels (Resende et al., 2010).

In this work, we have assessed the role of the limb signaling centers -AER and ZPA- on the dynamics of *hairy2* expression in the chick developing forelimb. We report that limb *hairy2* expression is an output of simultaneous FGF and SHH activities, with distinct temporal and spatial signaling properties. SHH creates a permissive state for *hairy2* expression by building up a proper ratio of Gli3-A and Gli3-R, in a long-term and long-range manner. FGF signaling, mediated by Erk and Akt pathway activation, plays an instructive role on *hairy2* expression with short-term/short-range characteristics. FGF instructive signal is only capable of mediating Erk/Akt phosphorylation and *hairy2* induction in a SHH-mediated permissive condition. Together, our results provide novel insights on temporally-regulated mechanisms operating in chick limb progenitor cells, by unveiling the requirement of integrated FGF and SHH signaling in time and space for cyclic *hairy2* expression.

Materials and Methods

Eggs and embryos

Fertilized *Gallus gallus* eggs were incubated at 37.8℃ in a 49% humidified atmosphere and staged according to Hamburger and Hamilton (HH) classification (Hamburger and Hamilton, 1992; reprint of 1951 paper). All the experiments were performed in stage HH22-24 forelimb buds.

Microsurgical ablation of AER and ZPA tissue

A window was cut in the shell of incubated eggs and the vitelline membrane was carefully removed. AER or ZPA was microsurgically ablated from the right wing bud of embryos using a tungsten needle. As a control, AER or ZPA extirpated embryos were randomly selected for direct fixation and hybridization with *fgf8* or *shh*, respectively. Operated embryos were re-incubated for different time periods (from 15 minutes to 22 hours), collected in PBS and fixed for *in situ* hybridization.

TUNEL assay

Apoptosis was analyzed using the Cell Death Detection Kit (Roche) in limb sections with and without AER or ZPA, after 2 and 6 hours of incubation, respectively. Ablated limbs were fixed overnight in 4% para-formaldehyde (PFA) in PBS, dehydrated, imbibed in paraffin and sliced into 6 µm sections using Microm HM325 on SuperFrost Plus (Menzel-Glaser) slides. Sections were rehydrated, permeabilized with Proteinase K treatment for 7.5 minutes at room temperature, and washed in PBS. Positive control embryos were incubated with DNase at 37℃ for 30 minutes. Sections were incubated for 2–4 hours at 37℃ with the TUNEL solution mix and washed at least three times in PBS before visualization.

Cell graft experiments

Clumps of QT6 quail fibroblasts stably transfected with an empty vector or with a construct carrying the SHH-coding region (QT6-SHH) (Duprez et al., 1998) were grafted in the posterior margin of the limb mesenchyme following ZPA ablation. Grafted embryos were re-incubated for 4–8 hours and processed for *in situ* hybridization.

Bead implantation experiments

Heparin acrylic beads (Sigma, H5263) and Affigel blue beads (Bio-Rad) were soaked for at least 1 hour at room temperature in recombinant human FGF8 or FGF2 (1 µg/µl; R&D Systems) and SHH (4 µg/µl; R&D Systems) protein solutions in PBS, respectively. The beads were implanted *in ovo* into the mesoderm of chick wing buds and beads soaked in PBS served as control. AG1-X2 beads (Bio-Rad) were incubated in SU5402 dissolved in DMSO (10 mM, Calbiochem). The MAPK inhibitor, U0126 (10 mM; Calbiochem) or the PI3K inhibitor, LY294002 (20 mM; Sigma) in DMSO was applied using Affigel blue beads as carrier. Respective beads soaked in DMSO served as control. Neither PBS nor DMSO control beads had any effect on gene expression.

In ovo treatments

5 µl of 1 mg/ml cyclopamine (Calbiochem) dissolved in 45% HBC (Sigma) in PBS was applied on top of the limb to specifically antagonize SHH signaling.

In situ hybridization and imaging

In situ hybridization was performed as previously described (Henrique et al., 1995), using antisense digoxigenin-labelled RNA probes: *shh* (Riddle et al., 1993), *hairy2* (Jouve et al., 2000), *fgf8* (Crossley et al., 1996) and *patched1* (Marigo and Tabin, 1996). Limbs processed for *in situ* hybridization were photographed using an Olympus DP71 digital camera coupled to an Olympus SZX16 stereomicroscope.

Immunoblot analysis

We performed western blot assays to analyze the intracellular pathways downstream of FGF signaling, namely ErK/MAPK and Akt/PI3K. We also assessed Gli3 activator and repressor, levels downstream of SHH signaling. FGF- or SHH-soaked beads were implanted in the desired forelimb bud domain and incubated for the desired period of time. Experimental and contralateral control limbs were surgically ablated and divided along the proximal–distal axis and the untreated halves were discarded. Portions from at least ten different limbs were collected and total protein was extracted from each pool of limbs, as previously described (Kling et al., 2002). 10 µg of protein extracts from FGF bead implanted limbs and the respective controls were loaded per well on a 12% SDS-PAGE minigel, subjected to electrophoresis at 100 V (room temperature) and transferred to Hybond-C extra membrane (Amersham Pharmacia Biotech, Inc., Piscataway, NJ). Blots were probed with p44/42 MAPK, phosphor-p44/42 MAPK, Akt, phosphor-Akt primary antibodies (Cell signaling) overnight at 4℃. β-tubulin (Abcam) antibody was used as loading control. Blots were incubated with anti-rabbit secondary antibody (Abcam) for 45 minutes at room temperature, developed with Super Signal West Femto Substrate (Pierce Biotechnology, Inc., Rockford, IL) and exposed in Chemidoc (Bio-Rad). Full length (activator) and the short form (repressor) of Gli3 were assessed using 70 µg of protein extract from FGF and SHH bead implanted limbs and the respective controls loaded per well in a 7% SDS-PAGE gel and the immunoblot was performed using a polyclonal antibody against Gli3, kindly provided by B. Wang (Wang et al., 2000). Each set of experiments were performed twice. Bands were quantified using Quantity one (Bio-Rad) and normalized with loading control (β-tubulin). For Gli3-A/Gli3-R ratio calculation, the proportion of Gli3-A in the experimental sample relative to total limb Gli3-A, was compared with its Gli3-R counterpart.

Results

Limb *hairy2* expression depends on AER-derived FGF signaling through Erk/MAPK and Akt/PI3K pathway activation

The developing limb presents distinct domains of *hairy2* expression (Fig. 1A), clearly visible from stages HH20 to HH28 (Pascoal et al., 2007): *hairy2* is persistently observed in the central muscle mass and in the posterior/distal limb mesenchyme, including the ZPA (PPD, posterior positive domain) and is absent from both the proximal posterior region (PND, posterior negative domain) and the anterior limb (AND, anterior negative domain). In the distal-most limb mesenchyme (DCD, distal cyclic domain), *hairy2* expression oscillates with a 6 hour periodicity (Pascoal et al., 2007) which, for the sake of simplicity, can be represented by three distinct phases (Fig. 1Ai–iii).

In order to evaluate if AER-derived signaling is involved in the regulation of distal limb *hairy2* expression, AER tissue was microsurgically ablated (-AER) from the forelimb of stage HH22-24 chick embryos *in ovo*, while the contralateral limb was untouched (control). Operated embryos were incubated for 4 hours, after which AER ablation was randomly confirmed by *fgf8* staining (Fig. 1Bi,ii) and *hairy2* expression was simultaneously evaluated in control and -AER limbs by *in situ* hybridization. We found that *hairy2* was totally abolished in both DCD and PPD, revealing a crucial role for AER signaling on

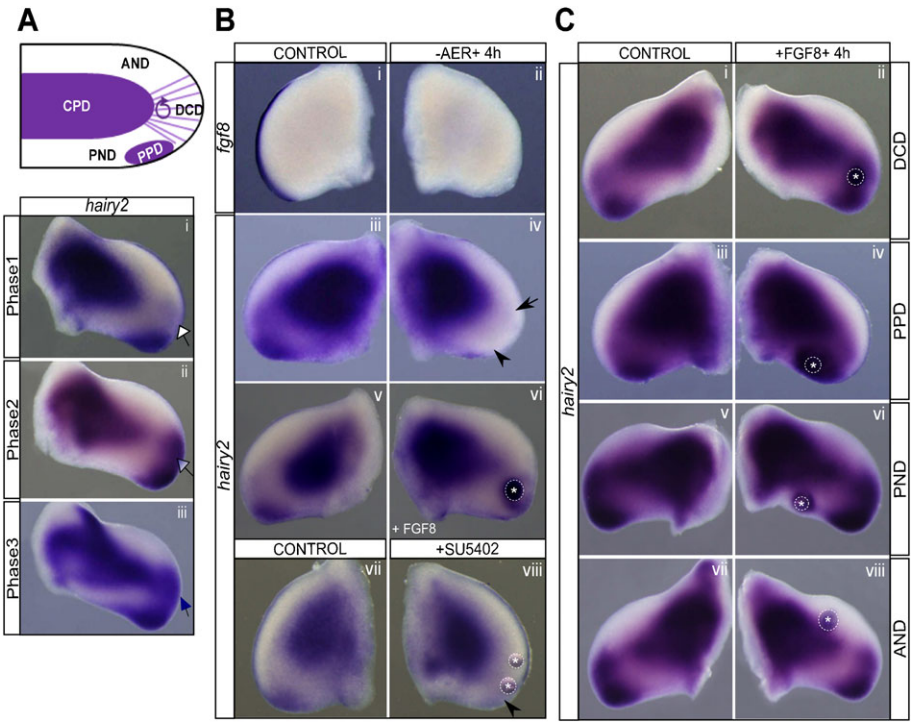

Fig. 1. AER-derived FGF signaling is required for limb *hairy2* expression. (**A**) Schematic representation of *hairy2* expression phases in HH24 chick forelimbs, cyclically recapitulated every 6 hours (Pascoal et al., 2007). *hairy2* is permanently present in the central positive domain (CPD) and in the posterior positive domain (PPD). It is not expressed in neither anterior negative (AND) nor posterior negative (PND) domains. *hairy2* is cyclically expressed in the distal cyclic domain (DCD), evidenced by different intensities in each expression phase (**Ai–iii**). Open, partially filled and filled arrows indicate absence, intermediate pattern and full *hairy2* expression in the DCD, respectively. (**Bi**,**ii**) *In situ* hybridization for *fgf8*, evidencing complete AER ablation. (**Biii–viii**) *hairy2* down-regulation upon AER ablation or SU5402 treatment (DCD, arrow; PPD, arrowhead), and *hairy2* induction by FGF8-bead in the absence of AER. (**C**) *hairy2* is up-regulated by implantation of FGF8-beads in all limb domains (**Ci–vi**), except the AND (**Cvii**,**viii**). Dorsal view; anterior to the top. *Beads, delimited by dashed lines.

hairy2 expression in these domains (Fig. 1Biii,iv; n=13/13). To interrogate if the observed effect was through FGF signaling, beads soaked in recombinant FGF8 or FGF2 were implanted in the DCD immediately following AER ablation, and *hairy2* expression was assessed after 4 hours of incubation. Both FGF2 and FGF8 were able to maintain *hairy2* expression around the beads (Fig. 1Bv,vi; FGF8: n=4/5; FGF2: n=3/3), supporting the requirement of FGFs for *hairy2* expression in the distal limb mesenchyme. Accordingly, treating the distal limb field with FGF inhibitor SU5402 (n=12) down-regulated (n=7/12) or even abolished (n=4/12) *hairy2* expression (Fig. 1Bvii,viii). FGF-mediated *hairy2* regulation was further assessed by implanting FGF8-beads in different distal limb domains. *hairy2* expression was enhanced in both DCD and PPD (Fig. 1Ci–iv; DCD: n=10/12; PPD: n=9/9) and up-regulated in the PND, a native *hairy2* negative domain (Fig. 1Cv,vi; n=25/27). Contrastingly, FGF8 was unable to induce *hairy2* in the AND (Fig. 1Cvii,viii; n=20/20), even after 20 hours of incubation and with increased amounts of FGF8 (supplementary material Fig. S1), indicating that the AND tissue is not competent to respond to FGF8 action on *hairy2*.

Erk/MAPK and Akt/PI3K are two predominant intracellular pathways functioning downstream of AER/FGF signaling in the chick limb (Kawakami et al., 2003). The activation levels of each pathway upon implantation of FGF8-soaked beads either in the AND or PND were assessed by western-blot (Fig. 2A). FGF8-bead implantation in the PND increased p-Erk levels by 77% and p-Akt by 37% (Fig. 2Ai,iii), suggesting that FGF-induced *hairy2* expression in the PND (Fig. 1Cv,vi) is mediated by Erk/MAPK and Akt/PI3K pathways. This was also confirmed by co-implanting FGF8 with beads soaked in specific MAPK or PI3K inhibitors (UO126 and LY294002, respectively). In fact, the tissue facing the MAPK or PI3K inhibitor source no longer exhibited ectopic *hairy2* (Fig. 2B) (U0126: n=4/4; LY294002: n=5/6). Contrastingly, FGF8-beads in the AND were unable to significantly activate Erk/MAPK or Akt/PI3K pathways and even resulted in decreased p-Akt levels (Fig. 2Ai,iii). In these conditions, no ectopic *hairy2* induction was observed (Fig. 1Cvii,viii), further substantiating Erk/Akt phosphorylation upstream of *hairy2* induction.

Together, our results indicate that AER-derived FGF is absolutely required, although not sufficient, for *hairy2* expression in the distal limb, mediated by Erk/MAPK and Akt/PI3K signaling pathways. They also reveal that AER/FGF does not activate downstream signaling pathways in a uniform fashion along the limb AP axis. In fact, we observed higher Erk phosphorylation levels in the posterior limb, when compared to the anterior region of control limbs (Fig. 2Ai,ii).

ZPA/SHH establishes the grounds for *hairy2* expression through Gli3 activity modulation

FGF8 was unable to induce *hairy2* in the AND, although it readily induced ectopic *hairy2* in the rest of the distal limb. This suggests the requirement of an additional signal, presumably present throughout all distal limb mesenchyme, except for the AND. SHH is a good candidate, since *hairy2* is persistently expressed in the PPD which presents high SHH levels produced by the ZPA, and is absent in SHH-deprived AND (Fig. 1A) (Wang et al., 2000; Harfe et al., 2004). A role for ZPA/SHH in the regulation of *hairy2* expression along the AP limb axis was thus assessed. Distal *hairy2* expression was abrogated following 6 hours of ZPA ablation *in ovo*, while AER/*fgf8* wasn't impaired (Fig. 3Ai–iv; *fgf8*: n=4/4; *hairy2*: n=22/27), strongly suggesting the requirement of ZPA-mediated signaling for *hairy2* expression. Replacing the ZPA by QT6 cells constitutively secreting SHH rescued *hairy2* (Fig. 3Av,vi; n=7/7), indicating that SHH is the ZPA-derived signal controlling *hairy2* expression. Supporting these results, treatment with the SHH inhibitor cyclopamine abolished *hairy2* in the distal limb

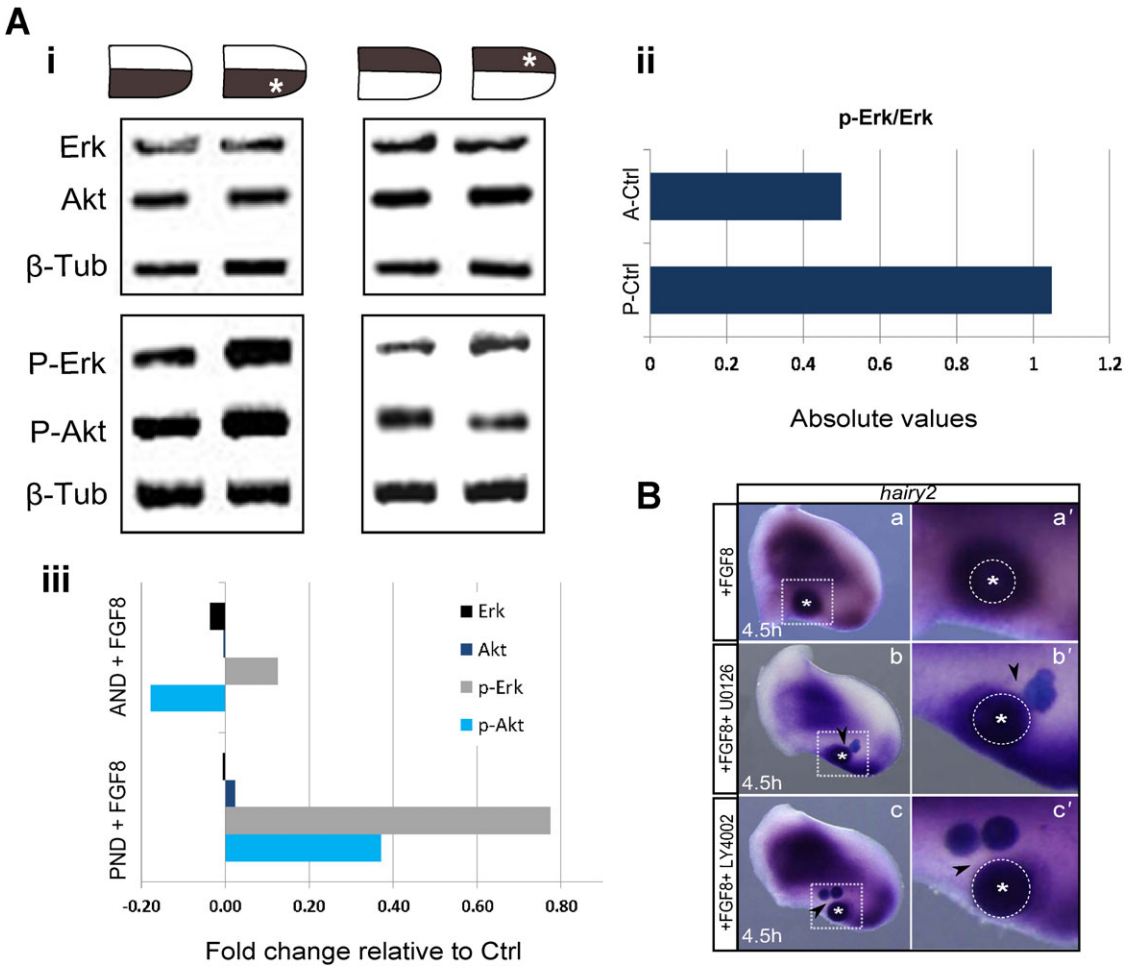

Fig. 2. Activation of Erk/MAPK and Akt/PI3K pathways mediates FGF-induced *hairy2* expression. (**Ai**) Immunoblots for Erk, p-Erk, Akt, p-Akt and β-tubulin (loading control) using total protein extracts from posterior or anterior FGF8-bead implanted limb halves and their contralateral controls, as schematically represented, after 4.5 hours of incubation. (**Aii**) Relative levels of Erk and p-Erk in the posterior and anterior control limb regions. (**Aiii**) Quantification of the fold change levels obtained in FGF-treated tissues relative to the posterior control. FGF8 significantly increases both p-Erk and p-Akt levels. (**B**) Inhibition of FGF8-induced *hairy2* expression by U0126 and LY4002 (MAPK and PI3K inhibitors, respectively). Arrowheads depict inhibition sites and delimited square areas in **a**,**b**,**c** are amplified in **a′**,**b′**,**c′**. Dorsal view; anterior to the top. *Beads, delimited by dashed lines.

(Fig. 3Bi,ii; n=5/6; supplementary material Fig. S2A,B). Noticeably, SHH-beads positioned in the AND resulted in an anterior expansion of *hairy2* (Fig. 3Biii,iv; n=11/15). These results clearly indicate that ZPA-derived SHH is essential for *hairy2* expression in the distal limb mesenchyme.

Gli3 is a major signal transducer of SHH signaling, being present in an activator form (Gli3-A) when SHH is present which prevents its proteolytic cleavage to Gli3-Repressor (Gli3-R) (Wang et al., 2000). In agreement with this, SHH-bead implantation in the AND resulted in an accumulation of Gli3-A (up to 76% increase), at the expense of the Gli3-R form (Fig. 3C,D). In this condition, there was ectopic *hairy2* induction (Fig. 3Biii,iv), contrarily to what was obtained when an FGF8-bead was implanted in the AND (Fig. 1Cvii,viii; supplementary material Fig. S1). FGF8 in the AND increased Gli3-R levels (Fig. 3C,D), suggesting that Gli3-R could be inhibiting *hairy2*. However, FGF8-bead in the PND also elevated the Gli3-R form (Fig. 3C,D) concomitantly with ectopic *hairy2* induction (Fig. 1Cv,vi), indicating that *hairy2* expression is not solely dependent on the presence or absence of Gli3-R. In fact, FGF8 in the PND increased both Gli3-R and Gli3-A to the same extent, evidencing that *hairy2* expression relies on balanced Gli3-A/Gli3-R activities. Accordingly, Gli3-A/Gli3-R in the control limb is higher in the posterior than in the anterior region (Fig. 3E), which coincides with the presence and absence of *hairy2* expression, respectively (Fig. 1A). This suggests the existence of a threshold of permissive Gli3-A/Gli3-R activity for *hairy2* expression along the limb AP axis.

We then analyzed the correlation between the experimental conditions leading to *hairy2* expression and Gli3-A/Gli3-R levels (Fig. 3E) and found a clear correlation between the presence/absence of *hairy2* expression and a value of Gli3-A/Gli3-R higher/lower than one, respectively (Fig. 3E). An FGF8-bead in the AND increased the Gli3-R form and slightly diminished Gli3-A levels, overall decreasing the Gli3-A/Gli3-R ratio and failing to induce *hairy2*. SHH, on the other hand, greatly increased Gli3-A/Gli3-R in the AND with concomitant *hairy2* induction. FGF8 in the PND maintained the Gli3-A/Gli3-R ratio of the posterior control limb and was able to induce ectopic *hairy2*. Together, these results show that SHH-mediated Gli3-A/Gli3-R>1 levels underlie the tissue's ability to respond to FGF8 for *hairy2* induction.

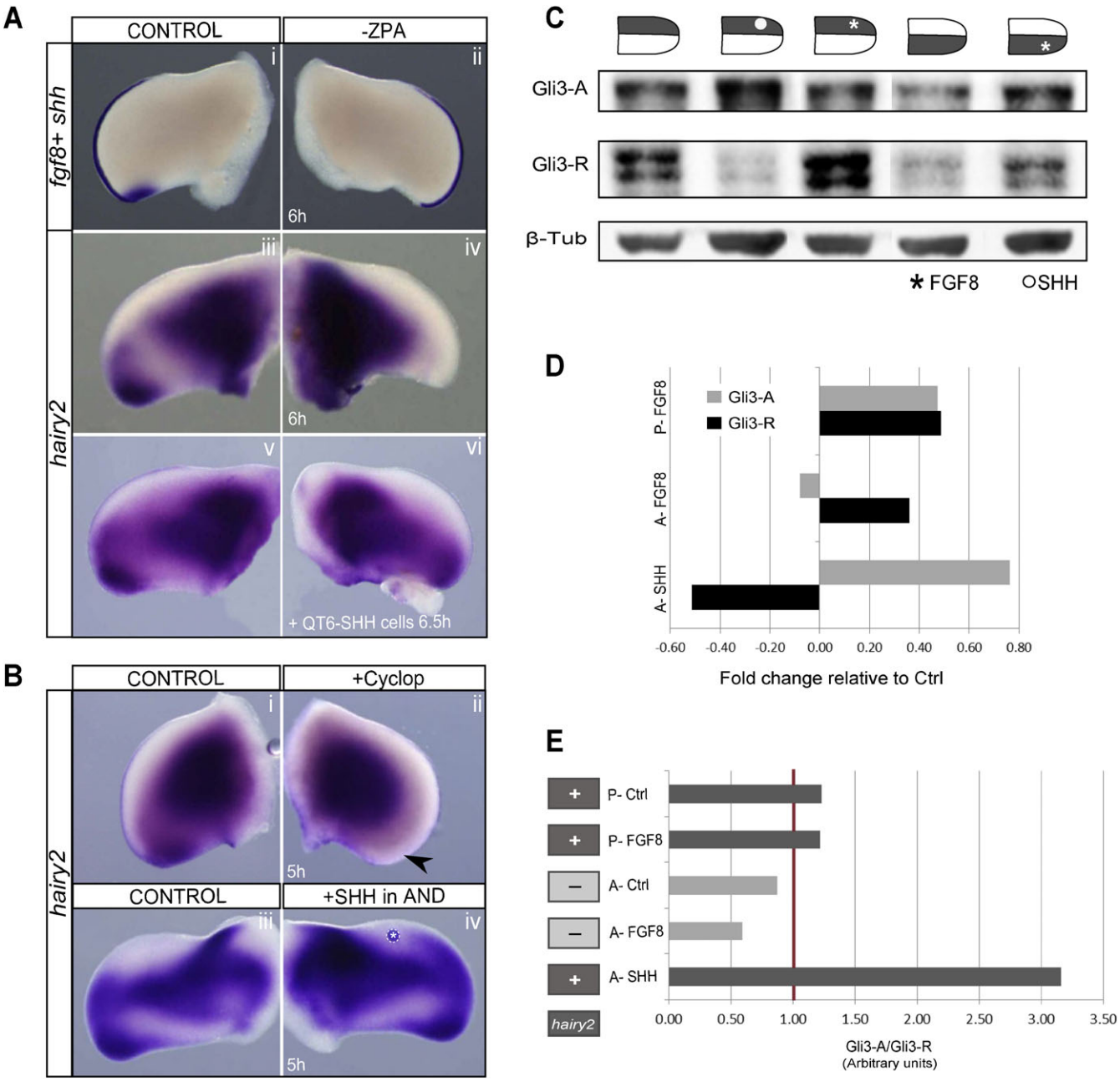

Fig. 3. ZPA/SHH establishes a permissive state for *hairy2* expression in the distal limb defined by balanced Gli3-A/Gli3-R levels. (**Ai**,**ii**) *In situ* hybridization for *fgf8* and *shh*, revealing ZPA ablation and unaffected AER/*fgf8* expression. (**Aiii–vi**) Distal *hairy2* expression is lost upon ZPA ablation and rescued by grafting SHH-secreting QT6-SHH cells. (**Bi**,**ii**) Cyclopamine abolishes *hairy2* expression in the distal limb (arrowhead). (**Biii**,**iv**) SHH-bead implantation in the AND ectopically expands *hairy2* expression. Dorsal view; anterior to the top. *Bead, delimited by dashed line. (**C**) Immunoblots for Gli3-A, Gli3-R and β-tubulin (loading control) using total protein extracts from SHH- (circle) or FGF8- (asterisks) treated anterior limb halves and posterior FGF8-bead implanted limb halves and their contralateral controls, as schematically represented, after 6 hours of incubation. (**D**) Fold change in the levels of Gli3-A and Gli3-R obtained in treated tissues. FGF8 increases both Gli3-A and Gli3-R to the same extent in the posterior limb (P-FGF8), whiles it only elevates Gli3-R in the anterior domain (A-FGF8). Here, SHH greatly increases Gli3-A, down-regulating Gli3-R (A-SHH). (**E**) Comparison of *hairy2* expression (+present; −absent) with different treatments and underlying ratio of Gli3-A/Gli3-R levels. *hairy2* is expressed only when the tissue presents Gli3-A/Gli3-R>1 (brown line), defining a SHH-mediated permissive state for *hairy2* expression.

Instructive-FGF and permissive-SHH cooperatively underlie *hairy2* expression in the distal limb mesenchyme

To further clarify the role of FGF and SHH on *hairy2* expression, we started by interrogating the ability of FGF8 to induce *hairy2* in the absence of the ZPA. FGF-beads implanted immediately upon ZPA ablation were still capable of locally inducing *hairy2* expression around the bead (Fig. 4Ai,ii; n=5/5). However, if the ZPA-ablated limbs were incubated for 6 hours prior to FGF-bead implantation, FGFs were no longer able to induce *hairy2* in neither the DCD (Fig. 4Aiii–iv; DCD: n=4/4) nor the PND (supplementary material Fig. S3). 6 hours was the incubation time previously found to be required for *hairy2* down-regulation

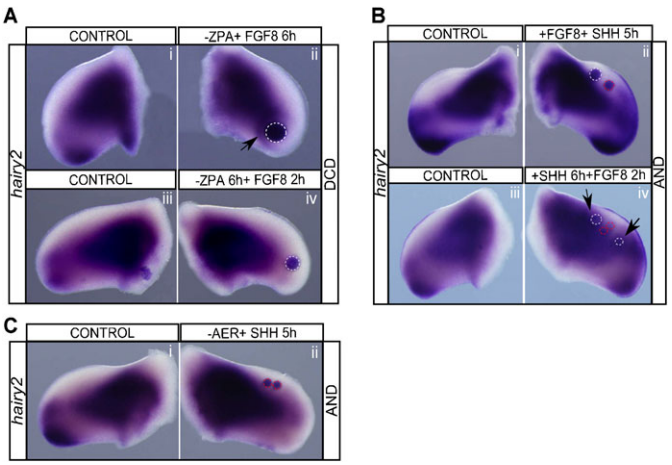

Fig. 4. Limb *hairy2* expression requires cooperative AER/FGF and ZPA/SHH signaling. (**A**) *hairy2* expression obtained upon implantation of FGF8-beads in ZPA-ablated limbs. Implantation of FGF8-bead immediately after ZPA ablation induces local *hairy2* expression (**Ai**,**ii**, arrow), but fails to do so after 6 hours of ZPA ablation (**Aiii**,**iv**). (**Bi**,**ii**) *hairy2* expression observed after co-implantation of FGF8 and SHH beads in the AND. Only the previously observed SHH-mediated expansion of *hairy2* expression is obtained. FGF beads implanted following 6 hours of SHH treatment are capable of inducing ectopic *hairy2* expression around the bead (**Biv**, arrows). (**Ci**,**ii**) SHH-bead is unable to induce *hairy2* upon AER ablation. SHH- and FGF8-beads are delimited by red and white dashed lines, respectively. Dorsal view; anterior to the top.

upon ZPA ablation (Fig. 3Aiii,iv), possibly corresponding to the time it takes for Gli3-A/Gli3-R ratio to fall under 1 due to the lack of SHH signaling. Furthermore, ectopic SHH in the AND never up-regulated *hairy2* locally around the bead even after 6 hours of incubation. Here, SHH-beads were only capable of expanding *hairy2* anteriorly along the tissue under direct AER/FGF influence (Fig. 3Biii,iv). It is thus highly unlikely that SHH plays an instructive role on *hairy2* expression. Instead, these results suggest that SHH is creating a permissive condition defined as Gli3-A/Gli3-R>1 (see previous section) for the action of a distinct, instructive signal emanated by the AER on *hairy2* expression. Reinforcing this idea, SHH was incapable of inducing *hairy2* in the AND upon AER ablation (Fig. 4Ci,ii; n=3/3; supplementary material Fig. S3).

In a complementary approach, we set out to determine if a permissive state could be imposed on the AND, and allow FGF8-mediated *hairy2* induction (supplementary material Fig. S1). When FGF8 and SHH-beads were concomitantly implanted in the AND, FGF8 did not induce *hairy2* around the bead and the overall result (Fig. 4Bi,ii; n=5/5) was indistinguishable from that obtained with a SHH-bead alone (Fig. 3Biii,iv). Whereas, when FGF8-bead was implanted in a limb previously incubated for 6 hours with SHH, allowing for the establishment of tissue permissiveness (Fig. 3E), it now induced ectopic *hairy2* (Fig. 4Biii,iv; n=6/6).

These experiments evidence that ZPA/SHH-mediated tissue permissiveness and AER/FGF instructive signals are both necessary for *hairy2* expression. Moreover, by carefully analyzing the time frame required for FGF/SHH effect on *hairy2* expression, we conclude that it does not involve a relay mechanism (supplementary material Fig. S4), but rather a convergence of signaling pathways in both time and space. The regulation of *hairy2* expression is a fine example of temporal and spatial cooperative action of the developing limb signaling centers.

Distinct temporal and spatial properties of AER/FGF and ZPA/SHH in distal limb *hairy2* expression regulation

To further understand the dynamics of *hairy2*'s dependence on AER/FGF and ZPA/SHH, a detailed study of the temporal response of *hairy2* expression to the removal of each limb signaling center was performed. In the absence of the AER, *hairy2* was down-regulated after 40 minutes (Fig. 5Ai,ii; n=2/2) and totally abolished upon 1 hour of incubation (Fig. 5Aiii,iv; n=5/5). This was not a consequence of cell death (supplementary material Fig. S5). Contrastingly, *hairy2* expression was not affected even after 2 hours of ZPA ablation (Fig. 5Av,vi; n=9/10), and cyclopamine-mediated SHH signaling inhibition for 4 hours only mildly down-regulated *hairy2* expression (supplementary material Fig. S2B). In fact, longer incubation periods were required for total *hairy2* depletion

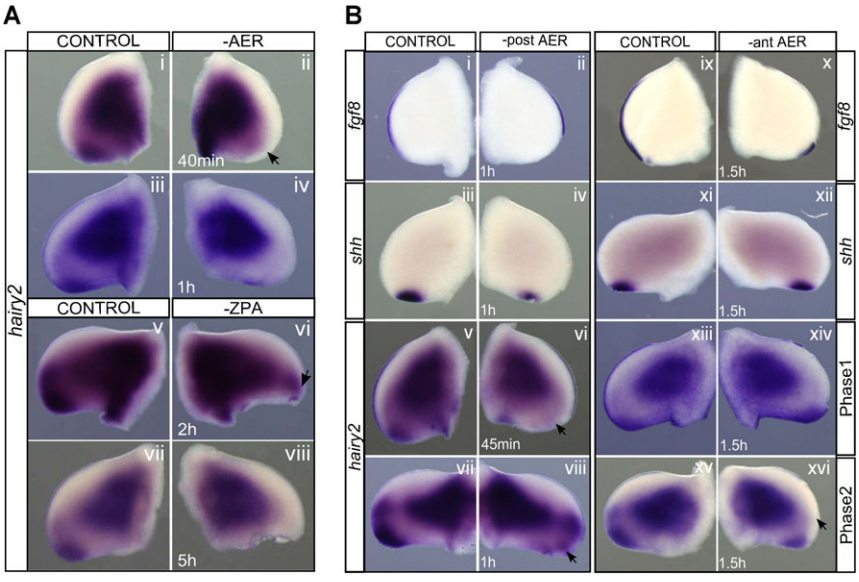

Fig. 5. AER/FGF and ZPA/SHH present different temporal and spatial modes of action on *hairy2* expression. (**A**) *hairy2* expression over time upon AER ablation and ZPA removal. AER ablation results in short-term down-regulation of *hairy2* (**Ai–iv**), while ZPA removal impacts *hairy2* only in a long-term fashion (**Av–viii**). Mild effects are observed at earlier time points (arrows). (**B**) AER/FGF signaling acts at short-range on *hairy2*. Upon partial ablation of either the posterior-AER (**Bi–viii**) or the anterior-AER (**Bix–xvi**), *hairy2* is down-regulated only in the tissue immediately adjacent to the ablation site (arrows). Partial ablations were confirmed by *fgf8* staining (Bi,ii,ix,x) and *shh* expression was assessed (Biii,iv,xi,xii). Dorsal view; anterior to the top.

in the distal mesenchyme after ZPA ablation (Fig. 5Avii,viii; n=22/27) or cyclopamine treatment (supplementary material Fig. S2B). This was not a consequence of impaired *fgf8* expression (Fig. 3Ai,ii; supplementary material Fig. S2A). Together, these data evidence different temporal responses of *hairy2* to both limb signaling centers: a short-term response to AER/FGF and long-term to ZPA/SHH.

To analyze the spatial effect of AER-mediated regulation on *hairy2* expression we proceeded to ablate solely the posterior- or anterior-AER, randomly confirmed by *fgf8* staining (Fig. 5Bi,ii,ix,x). Upon posterior-AER ablation, *hairy2* was rapidly abolished in the PPD (Fig. 5Bv–viii; Phase1: n=4/4; Phase2: n=2/2), while *shh* expression was still present (Fig. 5Biii,iv; n=2/2). This was a spatially restricted effect, since *hairy2* expression in the DCD remained unperturbed (Fig. 5Bvii,viii; n=2/2). Similarly, when the anterior-AER was ablated, *hairy2* was unperturbed in the posterior limb and abolished in the DCD (Fig. 5Bxiii–xvi; Phase1: n=2/2; Phase2: n=5/5). As expected, *shh* expression was present in this condition (Fig. 5Bxi,xii; n=2/2). Together, these results evidence a restricted spatial response of *hairy2* to AER signaling. On the contrary, ZPA ablation resulted in loss of *hairy2* expression in the entire distal limb mesenchyme (Fig. 3Aiii,iv), indicating a long-range effect on *hairy2* regulation. Replacement of the ZPA with QT6-SHH secreting cells, also rescued *hairy2* expression pattern along the whole distal limb AP-axis, further supporting a long-range signaling mode of action for ZPA/SHH on *hairy2*.

Altogether, our data propose ZPA/SHH and AER/FGF signaling as distinct regulatory mechanisms acting on distal limb *hairy2* expression, both temporally and spatially. SHH acts at a long-range and has a long-term permissive effect on *hairy2*, whereas the FGF effect is of a short-term, short-range instructive nature.

Discussion

The distal limb mesenchyme is under the influence of AER-derived FGFs and expresses appropriate FGF receptors (Sheeba et al., 2010). Applying complementary approaches, we found that AER/FGF8 plays an instructive role on limb *hairy2* regulation. In agreement, FGFs have also been reported to induce *HES* genes in other systems, such as somitogenesis (Dubrulle et al., 2001; Niwa et al., 2007), inner ear development (Doetzlhofer et al., 2009) and neural progenitor cells (Sanalkumar et al., 2010). We further identified Erk/MAPK and Akt/PI3K as the effectors of FGF-mediated *hairy2* regulation in the distal limb mesenchyme. FGF8 signaling is also mediated by Erk/MAPK and Akt/PI3K effectors during somitogenesis (Dubrulle and Pourquié, 2004; Delfini et al., 2005) and Erk phosphorylation is reported to underlie *HES* oscillations in the presomitic mesoderm (PSM) (Niwa et al., 2007; Niwa et al., 2011). A direct correlation between FGF-mediated Erk phosphorylation and *hairy2* mammalian homolog *hes1* expression has also been demonstrated in C3H10T1/2 cells (Nakayama et al., 2008).

The consistent absence of *hairy2* in the AND, despite of the exposure to endogenous or ectopic FGFs, indicates that FGF is not sufficient *per se* for *hairy2* expression. Furthermore, FGF8-beads in the AND were unable to activate Erk/MAPK or Akt/PI3K pathways, suggesting that this tissue is not competent to respond to FGF8, which is corroborated by different p-Erk levels observed in the anterior and posterior halves of the control limbs (Fig. 2Aii). Together, these observations allow us to postulate that the anterior limb is less responsive to FGF signaling compared to the posterior region and hints the need for an additional signal in the AND for *hairy2* induction. Accordingly, our data evidence a crucial role for ZPA/SHH in *hairy2* expression. Previous reports of SHH-mediated regulation of *hairy2* in somitogenesis (Resende et al., 2010), *hes1* in retina (Wall et al., 2009), mesodermal and neural cells (Ingram et al., 2008), further support our results. However, SHH alone is not sufficient for *hairy2* expression: SHH was unable to induce *hairy2* upon AER ablation (FGF source) and *hairy2* is absent from the PND limb domain, a SHH-signaling rich region which is distanced from the AER. Moreover, SHH-bead implantation in the AND, which is under AER/FGF influence, resulted in *hairy2* misexpression along the limb tissue strictly adjacent to the AER. Together, these observations reveal a clear cooperative action between FGF and SHH for *hairy2* induction. This mechanism does not involve a relay of FGF and SHH signals (supplementary material Fig. S4), but results from a parallel convergence of signaling activities, in both time and space. We reveal that SHH establishes a permissive state for FGF-instructive action on *hairy2* expression through fine-tuned Gli3-A/Gli3-R activity. FGF8 is capable of inducing *hairy2* expression when the proportion of Gli3-A exceeds that of Gli3-R (Gli3-A/Gli3-R>1) and cannot do so in the limb regions where Gli3-R activity prevails (Gli3-A/Gli3-R<1). These observations suggest that SHH signaling is providing a permissive condition for FGF8-mediated Erk/Akt phosphorylation and, hence, *hairy2* expression. Overall, we unveil Gli3-A/Gli3-R>1 as a SHH-mediated *sine qua non* condition for *hairy2* induction by FGF (Fig. 6A) and provide support to our previous proposal that SHH regulates PSM cyclic *hairy2* expression through Gli activity modulation (Resende et al., 2010). Using mouse Gli3 mutants, Wang et al. reported that the relative amount of Gli3 activator to repressor determines limb digit patterning along the distal AP axis (Wang et al., 2007). Despite of the proposal of a limb molecular oscillator by the long-standing Progress-Zone Model (Summerbell et al., 1973) and of the evidence of cyclic *hairy2* expression (Pascoal et al., 2007; Aulehla and Pourquié, 2008), a role for a limb molecular clock remains unclear (Towers et al., 2012). Nevertheless, it is tempting to speculate that *hairy2* expression dynamics established by joint FGF/SHH signaling may play a role in limb digit patterning.

In the course of our analysis we also uncovered that FGF and SHH pathways present distinct temporal and spatial signaling properties on *hairy2* expression in the distal limb, noticeably consistent with what would be expected for an instructive and permissive action, respectively. FGF8 impacted *hairy2* in a short-term manner (as early as 45 minutes) while effect of SHH signaling alteration on *hairy2* expression was only observed upon longer incubation periods (over 5 hours). In agreement, Harfe et al. showed that SHH-bead implantation in the anterior limb alters Gli3-R levels only after 4 hours of incubation (Harfe et al., 2004). Besides distinct temporal signaling dynamics, AER/FGF and ZPA/SHH exhibit distinguishing spatial regulatory actions on limb *hairy2* expression. We show that AER/FGF acts as a short-range signal on *hairy2*, possibly due to FGF interaction with heparin or heparan sulfate proteoglycans (Ornitz, 2000; Yu et al., 2009). Contrastingly, ZPA/SHH regulates *hairy2* at a distance, which is consistent with SHH-mediated limb AP axis patterning through long-range diffusion from the ZPA (Harfe et al., 2004).

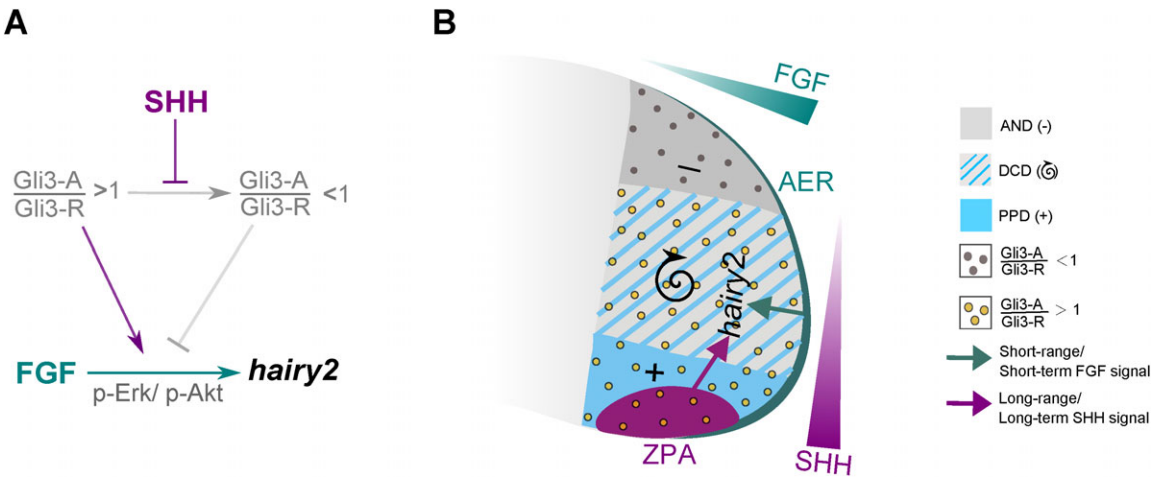

Fig. 6. Limb *hairy2* expression as a temporal and spatial output of joint FGF and SHH signaling. (**A**) High levels of instructive AER-derived FGF signaling, together with the Gli3-A/Gli3-R>1 permissive state established by ZPA/SHH, define the required conditions for *hairy2* expression. SHH acts as a long-term, long-range signal, ensuring a Gli3-A/Gli3-R>1 permissive state for *hairy2* expression. In these conditions, short-term/short-range FGF signaling is capable of inducing *hairy2* expression, acting as an instructive signal. (**B**) *hairy2* is expressed in the mesenchyme adjacent to AER/FGF and presents distinct expression domains: *hairy2* is persistently expressed in the posterior region overlapping the ZPA/SHH (PPD), is absent from the anterior limb (AND) and is cyclically expressed in the DCD. We describe FGF acting through Erk/MAPK and Akt/PI3K as an instructive signal for *hairy2* induction, in a short-term, short-range fashion throughout the distal limb mesenchyme. However, a permissive state mediated by SHH signaling is required for the tissue to respond to FGF inductive signal. SHH permissive signal is mediated by Gli3 activity and acts in a long-term, long-range manner and patterns *hairy2* expression along the distal limb AP axis. PPD and DCD present Gli3-A/Gli3-R above one (yellow dots), allowing sustained or oscillatory *hairy2* expression. In the AND, AER/FGFs can no longer induce *hairy2* since this tissue is in a non-permissive state: Gli3-A/Gli3-R below one (grey dots).

A positive feedback loop between FGF and SHH takes place during limb development (Zeller et al., 2009) and their joint requirement for the regulation of key molecules, such as *5′HoxD* genes, is known (Laufer et al., 1994; Niswander et al., 1994; Yang et al., 1997). Our present work describes distal limb *hairy2* as a unique molecular target of joint AER/FGF and ZPA/SHH action in both time and space. FGF/SHH-mediated regulation on *hairy2* does not involve a relay mechanism, operating in a uniquely short-framed temporal window, while reflecting distinctive temporal and spatial properties of AER- and ZPA-derived signaling (Fig. 6). Overall, AER-derived FGF signaling through Erk/Akt, together with graded levels of fine-tuned SHH-mediated Gli3-A/Gli3-R activity, give rise to different *hairy2* expression outcomes: persistent, cyclic or absent. Our results open the way for a better comprehension of a multitude of systems where FGF and SHH signaling pathways are involved and will further contribute to understand cyclic *HES* gene expression regulation in various processes that are also under joint FGF and SHH regulation, such as somitogenesis (Resende et al., 2010) neurogenesis (Shimojo et al., 2008; Sousa and Fishell, 2010) and stem cell pluripotency (Shi et al., 2008; Kobayashi et al., 2009).

Acknowledgements

The authors are grateful to Cheryll Tickle and Lewis Wolpert for helpful comments and critical reading of the manuscript, to Lisa Gonçalves and Tatiana Resende for fruitful discussions, Rute Moura and Paulina Piairo for technical assistance and Baolin Wang for the kind gift of Gli3 antibody. C.J.S. was supported by FCT, Portugal (grant SFRH/BD/33176/2007); R.P.A. is funded by Ciencia2007 Program Contract (Portuguese Government). This work was supported by research grants from IBB/CBME, LA to I.P., by FCT, Portugal (National and FEDER COMPETE Program funds: PTDC/SAU-OBD/099758/2008; PTDC/SAU-OBD/105111/2008, to I.P. and R.P.A., respectively) and EU/FP6 “Cells into Organs” Network of Excellence and IBB/CBME, LA, FEDER/POCI 2010.

Competing Interests

The authors have no competing interests to declare.

References

Ahn, S. and Joyner, A. L. (2004). Dynamic changes in the response of cells to positive hedgehog signaling during mouse limb patterning. *Cell* **118**, 505-516.

Andrade, R. P., Palmeirim, I. and Bajanca, F. (2007). Molecular clocks underlying vertebrate embryo segmentation: A 10-year-old *hairy*-go-round. *Birth Defects Res. C Embryo Today* **81**, 65-83.

Aulehla, A. and Pourquié, O. (2008). Oscillating signaling pathways during embryonic development. *Curr. Opin. Cell Biol.* **20**, 632-637.

Corson, L. B., Yamanaka, Y., Lai, K. M. and Rossant, J. (2003). Spatial and temporal patterns of ERK signaling during mouse embryogenesis. *Development* **130**, 4527-4537.

Crossley, P. H., Minowada, G., MacArthur, C. A. and Martin, G. R. (1996). Roles for FGF8 in the induction, initiation, and maintenance of chick limb development. *Cell* **84**, 127-136.

Delfini, M. C., Dubrulle, J., Malapert, P., Chal, J. and Pourquié, O. (2005). Control of the segmentation process by graded MAPK/ERK activation in the chick embryo. *Proc. Natl. Acad. Sci. USA* **102**, 11343-11348.

Dequéant, M. L., Glynn, E., Gaudenz, K., Wahl, M., Chen, J., Mushegian, A. and Pourquié, O. (2006). A complex oscillating network of signaling genes underlies the mouse segmentation clock. *Science* **314**, 1595-1598.

Doetzlhofer, A., Basch, M. L., Ohyama, T., Gessler, M., Groves, A. K. and Segil, N. (2009). *Hey2* regulation by FGF provides a *Notch*-independent mechanism for maintaining pillar cell fate in the organ of Corti. *Dev. Cell* **16**, 58-69.

Dubrulle, J. and Pourquié, O. (2004). *fgf8* mRNA decay establishes a gradient that couples axial elongation to patterning in the vertebrate embryo. *Nature* **427**, 419-422.

Dubrulle, J., McGrew, M. J. and Pourquié, O. (2001). FGF signaling controls somite boundary position and regulates segmentation clock control of spatiotemporal *Hox* gene activation. *Cell* **106**, 219-232.

Duprez, D., Fournier-Thibault, C. and Le Douarin, N. (1998). Sonic Hedgehog induces proliferation of committed skeletal muscle cells in the chick limb. *Development* **125**, 495-505.

Hamburger, V. and Hamilton, H. L. (1992). A series of normal stages in the development of the chick embryo. 1951. *Dev. Dyn.* **195**, 231-272.

Harfe, B. D., Scherz, P. J., Nissim, S., Tian, H., McMahon, A. P. and Tabin, C. J. (2004). Evidence for an expansion-based temporal Shh gradient in specifying vertebrate digit identities. *Cell* **118**, 517-528.

Henrique, D., Adam, J., Myat, A., Chitnis, A., Lewis, J. and Ish-Horowicz, D. (1995). Expression of a *Delta* homologue in prospective neurons in the chick. *Nature* **375**, 787-790.

Ingram, W. J., McCue, K. I., Tran, T. H., Hallahan, A. R. and Wainwright, B. J. (2008). Sonic Hedgehog regulates Hes1 through a novel mechanism that is independent of canonical Notch pathway signalling. *Oncogene* **27**, 1489-1500.

Jouve, C., Palmeirim, I., Henrique, D., Beckers, J., Gossler, A., Ish-Horowicz, D. and Pourquié, O. (2000). Notch signalling is required for cyclic expression of the hairy-like gene *HES1* in the presomitic mesoderm. *Development* **127**, 1421-1429.

Kawakami, Y., Rodríguez-León, J., Koth, C. M., Büscher, D., Itoh, T., Raya, A., Ng, J. K., Esteban, C. R., Takahashi, S., Henrique, D. et al. (2003). MKP3 mediates the cellular response to FGF8 signalling in the vertebrate limb. *Nat. Cell Biol.* **5**, 513-519.

Kling, D. E., Lorenzo, H. K., Trbovich, A. M., Kinane, T. B., Donahoe, P. K. and Schnitzer, J. J. (2002). MEK-1/2 inhibition reduces branching morphogenesis and causes mesenchymal cell apoptosis in fetal rat lungs. *Am. J. Physiol. Lung Cell. Mol. Physiol.* **282**, L370-L378.

Kobayashi, T., Mizuno, H., Imayoshi, I., Furusawa, C., Shirahige, K. and Kageyama, R. (2009). The cyclic gene *Hes1* contributes to diverse differentiation responses of embryonic stem cells. *Genes Dev.* **23**, 1870-1875.

Krol, A. J., Roellig, D., Dequéant, M. L., Tassy, O., Glynn, E., Hattem, G., Mushegian, A., Oates, A. C. and Pourquié, O. (2011). Evolutionary plasticity of segmentation clock networks. *Development* **138**, 2783-2792.

Laufer, E., Nelson, C. E., Johnson, R. L., Morgan, B. A. and Tabin, C. (1994). *Sonic hedgehog* and *Fgf-4* act through a signaling cascade and feedback loop to integrate growth and patterning of the developing limb bud. *Cell* **79**, 993-1003.

Marigo, V. and Tabin, C. J. (1996). Regulation of patched by sonic hedgehog in the developing neural tube. *Proc. Natl. Acad. Sci. USA* **93**, 9346-9351.

Nakayama, K., Satoh, T., Igari, A., Kageyama, R. and Nishida, E. (2008). FGF induces oscillations of Hes1 expression and Ras/ERK activation. *Curr. Biol.* **18**, R332-R334.

Niswander, L., Jeffrey, S., Martin, G. R. and Tickle, C. (1994). A positive feedback loop coordinates growth and patterning in the vertebrate limb. *Nature* **371**, 609-612.

Niwa, Y., Masamizu, Y., Liu, T., Nakayama, R., Deng, C. X. and Kageyama, R. (2007). The initiation and propagation of Hes7 oscillation are cooperatively regulated by Fgf and notch signaling in the somite segmentation clock. *Dev. Cell* **13**, 298-304.

Niwa, Y., Shimojo, H., Isomura, A., González, A., Miyachi, H. and Kageyama, R. (2011). Different types of oscillations in Notch and Fgf signaling regulate the spatiotemporal periodicity of somitogenesis. *Genes Dev.* **25**, 1115-1120.

Ornitz, D. M. (2000). FGFs, heparan sulfate and FGFRs: complex interactions essential for development. *Bioessays* **22**, 108-112.

Palmeirim, I., Henrique, D., Ish-Horowicz, D. and Pourquié, O. (1997). *Avian* hairy gene expression identifies a molecular clock linked to vertebrate segmentation and somitogenesis. *Cell* **91**, 639-648.

Pascoal, S., Carvalho, C. R., Rodriguez-León, J., Delfini, M. C., Duprez, D., Thorsteinsdóttir, S. and Palmeirim, I. (2007). A molecular clock operates during chick autopod proximal-distal outgrowth. *J. Mol. Biol.* **368**, 303-309.

Pourquié, O. (2011). Vertebrate segmentation: from cyclic gene networks to scoliosis. *Cell* **145**, 650-663.

Resende, T. P., Ferreira, M., Teillet, M. A., Tavares, A. T., Andrade, R. P. and Palmeirim, I. (2010). Sonic hedgehog in temporal control of somite formation. *Proc. Natl. Acad. Sci. USA* **107**, 12907-12912.

Riddle, R. D., Johnson, R. L., Laufer, E. and Tabin, C. (1993). *Sonic hedgehog* mediates the polarizing activity of the ZPA. *Cell* **75**, 1401-1416.

Sanalkumar, R., Indulekha, C. L., Divya, T. S., Divya, M. S., Anto, R. J., Vinod, B., Vidyanand, S., Jagatha, B., Venugopal, S. and James, J. (2010). ATF2 maintains a subset of neural progenitors through CBF1/Notch independent Hes-1 expression and synergistically activates the expression of Hes-1 in Notch-dependent neural progenitors. *J. Neurochem.* **113**, 807-818.

Sheeba, C. J., Andrade, R. P., Duprez, D. and Palmeirim, I. (2010). Comprehensive analysis of fibroblast growth factor receptor expression patterns during chick forelimb development. *Int. J. Dev. Biol.* **54**, 1517-1526.

Shi, Y., Sun, G., Zhao, C. and Stewart, R. (2008). Neural stem cell self-renewal. *Crit. Rev. Oncol. Hematol.* **65**, 43-53.

Shimojo, H., Ohtsuka, T. and Kageyama, R. (2008). Oscillations in notch signaling regulate maintenance of neural progenitors. *Neuron* **58**, 52-64.

Sousa, V. H. and Fishell, G. (2010). Sonic hedgehog functions through dynamic changes in temporal competence in the developing forebrain. *Curr. Opin. Genet. Dev.* **20**, 391-399.

Sparrow, D. B., Chapman, G., Smith, A. J., Mattar, M. Z., Major, J. A., O'Reilly, V. C., Saga, Y., Zackai, E. H., Dormans, J. P., Alman, B. A. et al. (2012). A mechanism for gene-environment interaction in the etiology of congenital scoliosis. *Cell* **149**, 295-306.

Summerbell, D., Lewis, J. H. and Wolpert, L. (1973). Positional information in chick limb morphogenesis. *Nature* **244**, 492-496.

Towers, M. and Tickle, C. (2009). Growing models of vertebrate limb development. *Development* **136**, 179-190.

Towers, M., Wolpert, L. and Tickle, C. (2012). Gradients of signalling in the developing limb. *Curr. Opin. Cell Biol.* **24**, 181-187.

Turnpenny, P. D., Alman, B., Cornier, A. S., Giampietro, P. F., Offiah, A., Tassy, O., Pourquié, O., Kusumi, K. and Dunwoodie, S. (2007). Abnormal vertebral segmentation and the notch signaling pathway in man. *Dev. Dyn.* **236**, 1456-1474.

Wall, D. S., Mears, A. J., McNeill, B., Mazerolle, C., Thurig, S., Wang, Y., Kageyama, R. and Wallace, V. A. (2009). Progenitor cell proliferation in the retina is dependent on Notch-independent Sonic hedgehog/Hes1 activity. *J. Cell Biol.* **184**, 101-112.

Wang, B., Fallon, J. F. and Beachy, P. A. (2000). Hedgehog-regulated processing of Gli3 produces an anterior/posterior repressor gradient in the developing vertebrate limb. *Cell* **100**, 423-434.

Wang, C., Rüther, U. and Wang, B. (2007). The Shh-independent activator function of the full-length Gli3 protein and its role in vertebrate limb digit patterning. *Dev. Biol.* **305**, 460-469.

William, D. A., Saitta, B., Gibson, J. D., Traas, J., Markov, V., Gonzalez, D. M., Sewell, W., Anderson, D. M., Pratt, S. C., Rappaport, E. F. et al. (2007). Identification of oscillatory genes in somitogenesis from functional genomic analysis of a human mesenchymal stem cell model. *Dev. Biol.* **305**, 172-186.

Yang, Y. and Niswander, L. (1995). Interaction between the signaling molecules WNT7a and SHH during vertebrate limb development: dorsal signals regulate anteroposterior patterning. *Cell* **80**, 939-947.

Yang, Y., Drossopoulou, G., Chuang, P. T., Duprez, D., Marti, E., Bumcrot, D., Vargesson, N., Clarke, J., Niswander, L., McMahon, A. et al. (1997). Relationship between dose, distance and time in *Sonic Hedgehog*-mediated regulation of anteroposterior polarity in the chick limb. *Development* **124**, 4393-4404.

Yu, S. R., Burkhardt, M., Nowak, M., Ries, J., Petrásek, Z., Scholpp, S., Schwille, P. and Brand, M. (2009). Fgf8 morphogen gradient forms by a source-sink mechanism with freely diffusing molecules. *Nature* **461**, 533-536.

Zeller, R., López-Ríos, J. and Zuniga, A. (2009). Vertebrate limb bud development: moving towards integrative analysis of organogenesis. *Nat. Rev. Genet.* **10**, 845-858.